Kinetics of Intramembrane Charge Movement and Sodium Current in Frog Node of Ranvier

JEAN MARC DUBOIS and MARTIN F. SCHNEIDER

From the Laboratoire de Neurobiologie, Ecole Normale Supérieure, 46, rue d'Ulm, 75005 Paris, France; and the Department of Physiology, University of Rochester School of Medicine and Dentistry, Rochester, New York 14642

ABSTRACT Intramembrane charge movement (Q) and sodium current (I_{Na}) were monitored in isolated voltage-clamped frog nodes of Ranvier. ON charge movements (Q_{ON}) for pulses from the holding potential (−100 mV) to potentials $V \leq 0$ mV followed single exponential time courses, whereas two exponentials were found for pulses to $V \geq 20$ mV. The voltage dependence of both Q_{ON} and its time constant τ_{ON} indicated that the two ON components resolved at $V \geq 20$ mV were also present, though not resolvable, for pulses to $V \leq 0$ mV. OFF charge movements (Q_{OFF}) monitored at various potentials were well described by single exponentials. When Q_{OFF} was monitored at −30 or −40 mV after a 200-μs pulse to +20 mV and Q_{ON} was monitored at the same potential using pulses directly from −100 mV, $\tau_{ON}/\tau_{OFF} = 2.5 \pm 0.3$. At a set OFF potential (−90 to −70 mV), τ_{OFF} first increased with increasing duration t_{ON} of the preceding pulse to a given potential (0 to +30 mV) and then decreased with further increases in t_{ON}. The declining phase of τ_{OFF} followed a time course similar to that of the decline in Q_{OFF} with t_{ON}. For the same pulse protocol, the OFF time constant τ_{Na} for I_{Na} also first increased with t_{ON} but then remained constant over the t_{ON} interval during which τ_{OFF} and Q_{OFF} were declining. After 200- or 300-μs pulses to +20, +30, or +50 mV, τ_{OFF}/τ_{Na} at −70 to −90 mV was 1.2 ± 0.1. Similar τ_{OFF}/τ_{Na} ratios were predicted by channel models having three identical charged gating particles that can rapidly and reversibly form an immobile dimer or trimer after independently crossing the membrane from their OFF to their ON locations.

INTRODUCTION

In the original characterization of the voltage- and time-dependent ionic conductance changes that underlie the squid axon action potential, Hodgkin and Huxley (1952) suggested that the conductance state of individual membrane ionic channels might be determined by the intramembrane location of charged or dipolar molecules that could change position or orientation in response to changes in membrane electric field. Some 20 years later, charge displacement currents presumably due to movement of intramembrane

J. GEN. PHYSIOL. © The Rockefeller University Press · 0022-1295/82/04/0571/32 $1.00 571
Volume 79 April 1982 571-602

charges were recorded from both muscle fibers (Schneider and Chandler, 1973) and nerve axons (Armstrong and Bezanilla, 1973). Most of the intramembrane charge movement recorded from axons appears to be related to sodium channels (Yeh and Armstrong, 1978; Cahalan and Almers, 1979; Almers, 1978).

It is now generally agreed (Armstrong and Bezanilla, 1974; Neumcke et al., 1976; Keynes, 1980) that gating current is not simply proportional to the rate of change of the *m* parameter in the Hodgkin-Huxley (1952) model. Although alternative models for sodium channel gating have been suggested (cf. Armstrong, 1978), none has as yet been exhaustively tested. The present report represents an attempt to quantitatively characterize various kinetic properties of intramembrane charge movement and sodium current in frog node of Ranvier. Any satisfactory model for sodium channel gating in node should be capable of accounting for and reproducing such observations.

An abstract of some of the present results was presented to the VII International Biophysics Congress (Schneider and Dubois, 1981).

METHODS

Experiments were carried out on nodes of Ranvier in isolated myelinated nerve fibers from the frog *Rana esculenta*. Fibers were bathed in Ringer's solution for dissection and mounting in the experimental chamber. The end pools were then changed to isotonic CsCl (120 mM) and both fiber ends were recut. Isotonic CsCl was used at the cut ends during all experiments unless otherwise specified. The Ringer's solution contained 111.5 mM NaCl, 2.5 mM KCl, 1.8 mM $CaCl_2$, and 2.4 mM $NaHCO_3$, and its pH was 7.4. Ionic current through potassium channels was suppressed by the internal cesium (Dubois and Bergman, 1975) and by 10 mM tetraethylammonium (TEA) ion (Hille, 1967; Koppenhöfer, 1967) added as TEA chloride to the Ringer's solution bathing the node. All results were obtained at 8–12°C.

The nodal membrane was voltage-clamped using the method of Nonner (1969). Membrane currents were calculated arbitrarily assuming an exoplasmic resistance of 10 MΩ. A membrane potential of −70 mV was defined as that potential corresponding to 30% "fast" inactivation of the sodium current (Nonner et al., 1975). The nodes were routinely maintained at a holding potential of −100 mV. For each voltage pulse, the time-independent linear leakage currents and two components of exponentially decaying linear capacity current were approximated by an analog circuit driven by the command pulse (Dubois and Bergman, 1977*a*) and were subtracted from the total current by a differential amplifier.

Sodium currents (I_{Na}) were obtained after low-pass filtering with an active Bessel filter with cut-off frequency set at 20, 30, or 40 kHz. Residual linear current components were generally removed by digitally summing currents for a given number of depolarizing pulses of amplitude P with those for twice that number of hyperpolarizing pulses of amplitude −P/2. This protocol will be referred to as the "−P/2 routine." Whenever the depolarizing pulse had multiple steps, each step was present at half amplitude in −P/2. Both P and −P/2 were applied from the holding potential.

Charge movement was recorded after blocking ionic current through sodium channels by also adding 10^{-6} M tetrodotoxin (TTX) to the Ringer's solution bathing the node. To minimize noise and obtain direct estimates of charge transfer, the current remaining after subtracting linear components was integrated by an operational

amplifier circuit. The integrated signal was digitized and summed as for I_{Na}, but without prior filtering. To minimize drift and prevent saturation, the operational amplifier integrator was AC-coupled at its input (600 Hz) and its feedback capacitor was shunted until 0.5 ms before the start of each record using a transistor switch. Charge movement records were routinely obtained using 24 depolarizing pulses in the −P/2 routine. To estimate possible errors in Q due to the apparatus, tests were carried out using a dummy circuit representing the nerve fiber and external resistances. For a 1-ms pulse P that moved 100 fC of charge, the mean ± SEM charge remaining after the −P/2 routine was 1.8 ± 0.3 fC (N = 50; maximum = 6 fC).

Analog-to-digital conversion (8-bit) and digital summing (16-bit capacity) were carried out by a single averager (Memoscope RE10; R2E, Orsay, France) that sampled 1,000 successive points at 4-μs intervals. In the few experiments in which I_{Na} inactivation during a pulse was monitored, 16-μs sampling intervals were used. After completion, each sum record was converted to analog form, displayed on an oscilloscope, and photographed. The photographed records were subsequently projected and traced continuously by hand because individual points were not resolvable over most of the record. Such tracings were then measured at 12.5- or 25-μs intervals to give the data actually analyzed. Time constants and initial amplitudes of apparently exponential components were determined by a linear regression analysis (9810A; Hewlett-Packard Co., Palo Alto, Calif.) using logs of the measured values. Sodium tail current records obtained with the −P/2 routine generally appeared to be distorted during the initial 25 or 35 μs, perhaps due to oscillation or amplifier saturation, so that the 37.5- or 50-μs value was the first used in analyzing I_{Na} tails. For the same fibers in TTX, charge movement records obtained with the same pulses but using integrated currents appeared to have less initial distortion and were analyzed starting either 12.5 or 25 μs after pulse ON or OFF.

RESULTS

Direct Recording of Charge Movement

Various types of recordings of gating current (I_Q) or its associated gating charge movement (Q) for a given pulse are illustrated in Fig. 1. Trace *a* is a standard recording of gating current, obtained here using the −P/2 routine. It shows a transient outward current during the pulse and transient inward current after the pulse. The fact that the steady current during the pulse was below the initial baseline indicates a slightly lower conductance for the depolarizing than for the hyperpolarizing pulses. Gating current is assumed to constitute all current above this steady level during the pulse and all current after the pulse. Trace *b* of Fig. 1 was obtained for pulses to the same potentials as in *a*, but by using analog integration before digitization and summing by the −P/2 routine. As expected for the integral of I_Q, trace *b* rose at pulse ON and fell at pulse OFF. After its initial rising phase, trace *b* declined approximately linearly with time during the pulse. This also was to be expected because the current record (trace *a*) had a negative steady "ON" level that, when integrated, would produce a linearly declining phase. Trace *b* was corrected for time-independent nonlinear currents by fitting straight sloping baselines by eye to the latter parts of its ON and OFF segments, extrapolating the baselines to the preceding pulse edge, and subtacting them from *b* to give *c*. The fact that trace *c* does not return to the initial baseline after the pulse

illustrates the well-established finding that the charge carried by ON gating current exceeds that carried back by OFF gating current if the OFF potential is not considerably negative to −100 mV (Armstrong and Bezanilla, 1977; Nonner et al., 1978).

In principle, gating current and gating charge movement traces contain the same information. For the pulse used in Fig. 1, OFF gating current in node of

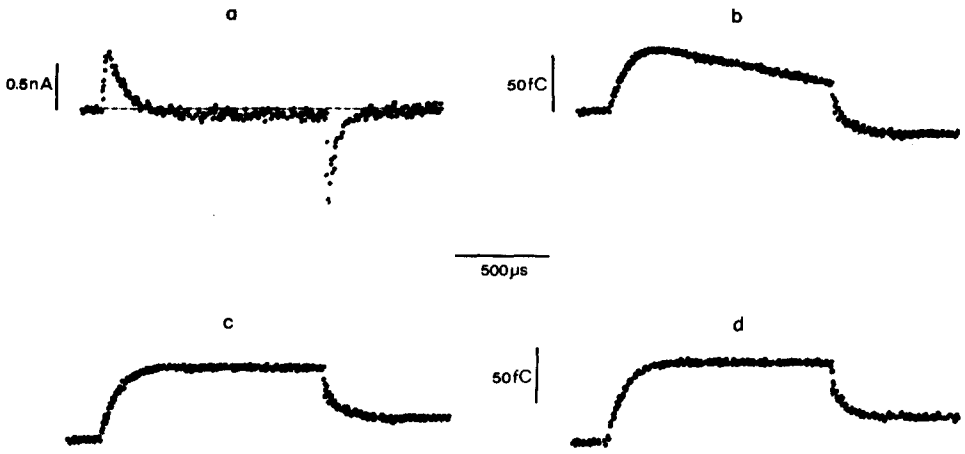

FIGURE 1. Gating current and gating charge movement traces. (*a*) Gating current recorded in response to 24 120-mV depolarizing pulses and 48 60-mV hyperpolarizing pulses (−P/2 routine). (*b*) Gating charge movement recorded in response to 24 120-mV depolarizing pulses and 48 60-mV hyperpolarizing pulses (−P/2 routine). (*c*) Gating charge movement trace presented in *b* after correction for time-independent nonlinear currents. (*d*) Gating charge movement recorded in response to 24 120-mV depolarizing pulses and 24 120-mV hyperpolarizing pulses and corrected for time-independent nonlinear currents. Temperature: 11°C. Fiber: 8-1-80.

Ranvier is well described by a single exponentially decaying component (Neumcke, et al., 1976; Dubois and Bergman, 1977*b*) so that

$$I_Q(t) = I_Q(0)\exp(-t/\tau_Q), \tag{1}$$

where t is time and τ_Q is the gating current time constant. The gating charge movement is by definition the integral of the gating current so that if Eq. 1 described $I_Q(t)$, then $Q(t)$ will be

$$Q(t) = \tau_Q I_Q(0)[1 - \exp(-t/\tau_Q)]. \tag{2}$$

$Q(t)$ thus rises to its final level $\tau_Q I_Q(0)$ along a single exponential time course having the same time constant as the decline of $I_Q(t)$. If I_Q were to be composed of multiple exponential components with different $I_Q(0)$ and τ_Q values but with each following Eq. 1, then Q would also be composed of the same number of components, each following Eq. 2 with corresponding $I_Q(0)$ and τ_Q. Similar equations apply to the OFF charge except that the initial value of Q is nonzero.

Eqs. 1 and 2 allow quantitative comparison of I_Q and Q records for a given pulse. Considering traces *a* and *c* in Fig. 1, the ON τ_Q values obtained from the I_Q and Q traces were 92 and 87 μs, and the final Q_{ON} values were 83 fC for $\tau_Q I_Q(0)$ from I_Q and 80 fC from Q. Other paired I_Q and Q records showed similarly good agreement of parameters. Since the Q traces were considerably less noisy than I_Q, they were used for the studies presented here. Gating current in node has previously been analyzed using Q traces generated from digital I_Q records (Neumcke et al., 1976; Nonner et al., 1978).

Trace *d* of Fig. 1 presents a control for nonlinear charge displacement over the voltage range negative to −100 mV. It was obtained from currents for the same size depolarizing pulses as in *c* but here summed with currents for the same number of hyperpolarizing pulses of equal amplitude (± P routine). The similarity of *c* and *d* and of other pairs of records comparing the −P/2 and ±P routines indicates that charge movement recordings are minimally influenced by nonlinearities in the hyperpolarizing voltage range. To minimize the possibility of membrane damage by large hyperpolarizing pulses, charge movements were generally recorded with the −P/2 routine. The ±P routine was used for a few fibers that were found to tolerate large hyperpolarizing pulses.

Two Components of ON Charge Movement

ON charge movement records obtained by the integral method for pulses to several different membrane potentials in the same fiber are presented in the upper part of Fig. 2. In the lower part of Fig. 2 the Q_{ON} time courses are analyzed using normalized semilog plots of the fraction $1 - [Q_{ON}(t)/Q_{ON}(\infty)]$ of ON charge remaining to be moved for each record. For depolarizing pulses to and below 0 mV, the ON charge movement is well described by a single exponential, whereas for pulses to and beyond +20 mV, two exponential components are required. The single integrated ON displacement current record at a positive potential presented by Neumcke et al. (1976, Fig. 3D) deviates appreciably from its single exponential fit and thus also indicates the presence of more than one component of Q_{ON} at positive potentials in node of Ranvier. After correcting I_{Na} turn-on in one fiber for a two-exponential inactivation process in parallel (Chiu, 1977), I_{Na} activation at +20 mV approached its final level at about the same time as the slow component of Q_{ON} in the same fiber. This would tend to indicate that the present slow component of Q_{ON} may be similar to the "intermediate" component in squid axons (Armstrong and Gilly, 1979) rather than the squid axon "slow" component (Armstrong and Bezanilla, 1977).

The charge-voltage relationship for the experiment of Fig. 2 is analyzed in Fig. 3A. The filled circles present values of total Q_{ON} as a function of pulse membrane potential. At positive potentials the amounts of charge carried by the fast (squares) and slow (triangles) kinetically separable components are also indicated. The values of total Q_{ON} at 0 mV are larger than the Q values for either the fast or the slow components at positive potentials. Therefore, if there were only a single component of Q for pulses to and below 0 mV and if a second component began to contribute to Q only for pulses beyond 0 mV,

the charge moved by the first component would have to attain a maximum at about 0 mV and then decline for pulses beyond 0 mV. Such behavior would not be expected for a voltage-dependent redistribution of charges or dipoles within the membrane. A more likely hypothesis is that there are multiple components of charge movement even at negative potentials but that their time constants are too similar to allow kinetic separation using these data and techniques.

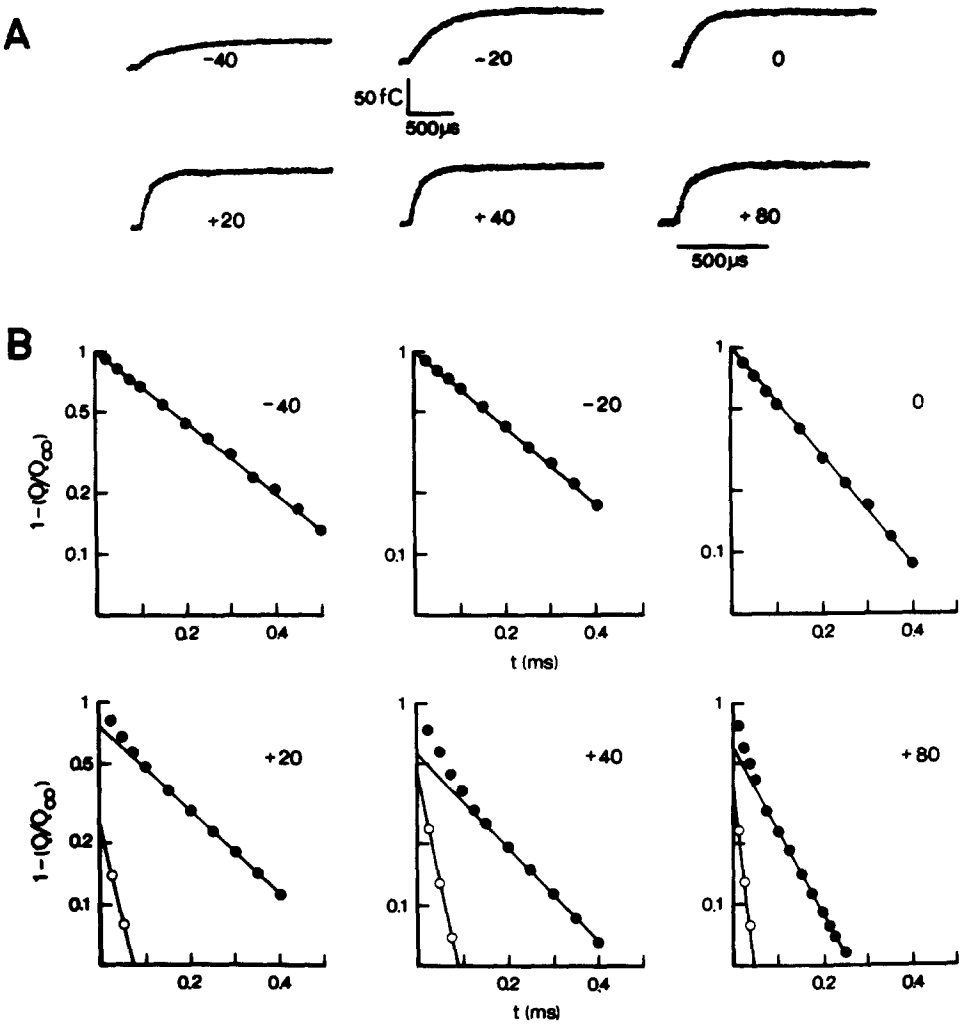

FIGURE 2. ON charge movement kinetics. (A) Traces of charge movement recorded at different membrane potentials and corrected for time-independent nonlinear currents. (B) Semilogarithmic plots of charge movement traces presented in part A. Filled circles give the overall charge movement and open circles (for pulses to and beyond +20 mV) give the charge movement remaining after subtracting the slow exponential component (straight lines through filled circles). Temperature: 8°C. Fiber: 10-4-80.

The relationship between τ_{ON} and pulse membrane potential (Fig. 3B) for the experiment of Figs. 2 and 3A appears to be consistent with the latter hypothesis. Within the scatter in the data, neither the faster nor the slower of the two time constants at and beyond +20 mV appears to continue the trend of the voltage dependence of the single time constants observed up to 0 mV.

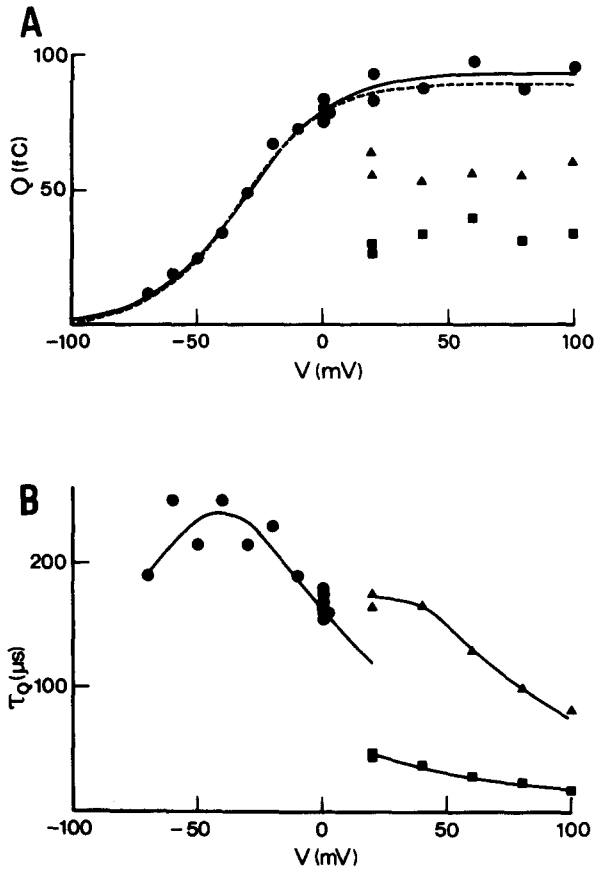

FIGURE 3. Voltage dependence of ON charge movement. (A) ON charge movement vs. voltage relationship. The circles represent the overall charge movement. For membrane potentials equal to and more positive than +20 mV, the triangles and squares represent, respectively, the slow and fast charge movement components. The curves present the nonlinear least-squares fit of Eq. 3 to all data points (solid curve) or to only the data points at or below 0 mV (dashed curve). Parameter values obtained from the fits were Q_{max} = 100 or 96 fC, $\bar{V}$ = −31.6 or −33.4 mV, and k = 18.1 or 16.8 mV for the solid or dashed curves, respectively. (B) ON charge movement time constants vs. voltage. For membrane potentials more negative than +20 mV, the charge movement kinetics were described by one exponential (circles). For membrane potentials equal to or more positive than +20 mV, the charge movement kinetics were described by the sum of a slow (triangles) and a fast (squares) exponential component. Curves were drawn by eye. Same fiber and run as for Fig. 2.

Thus neither of the two components at positive potentials appears to correspond to a single process occurring at and below 0 mV.

Table I presents values of time constants and relative amplitudes for the two ON charge movement components resolved for pulses to +20 mV in four fibers. Based on exponential extrapolation to pulse ON, the slow component carried 0.66 ± 0.04 (mean ± SEM) of the total Q_{ON} at +20 mV. It should be noted that this charge assignment assumes that both components of Q_{ON} follow exponential time courses without delay. If the slow component actually began only after a delay, as suggested by Armstrong and Gilly (1979) for the intermediate component in squid axons, we would be overestimating the charge transfer caused by the slow component and underestimating that caused by the fast component. In one of the fibers in Table I, Q_{ON} was also monitored for pulses to 0 mV and found to be well described by a single exponential. In this fiber the mean value of Q_{ON} at 0 mV was 87% of Q_{ON} at +20 mV (Fig. 3A).

TABLE I

TIME CONSTANTS AND RELATIVE AMOUNTS OF TWO COMPONENTS OF ON CHARGE MOVEMENT AT +20 mV

Fiber	N*	Q_{slow}/Q_{total}	τ_{fast}	τ_{slow}
			μs	μs
11-4-80	4	0.75	65	180
28-4-80	3	0.63	80	220
10-4-80	2	0.66	43	170
21-2-80A	6	0.58	52	152
Mean±SEM		0.66±0.04	60±8	180±14

* Number of records of Q_{ON} at +20 mV analyzed to give the mean values presented for each fiber.

The solid line in Fig. 3A presents the nonlinear least-squares fit (Horowicz and Schneider, 1981*a*) of the total Q_{ON} data by the equation

$$Q_{ON} = Q_{max}/[1 + \exp(\bar{V}\text{-}V)/k] \quad (3)$$

for the steady-state transfer of charge due to redistribution of charged intramembrane particles between two sites according to the Boltzmann relationship (Schneider and Chandler, 1973; Keynes and Rojas, 1974; Nonner et al., 1975). The adjusted parameters were the maximum charge displaced Q_{max}, the membrane potential for 50% charge displacement $\bar{V}$ and the steepness factor k (equal to $RT/\alpha z$, with R being the gas constant, T the absolute temperature, z the valence of the charged particle, and α the fraction of the membrane field that the particles traverse). The fact that Eq. 3, which describes a single charge transition, can closely approximate the Q vs. V data does not rule out the possibility of multiple Q components. Horowicz and Schneider (1981*b* and unpublished calculations) have found that Q vs. V relationships predicted for a variety of multi-transition models for charge movement may be experimen-

tally indistinguishable from Eq. 3. When Eq. 3 was fit only to the data points at or below 0 mV in Fig. 3A, the theoretical curve (dashed line) was quite close to the one obtained when all points were considered. This also tends to argue against a second Q component appearing only for pulses to positive potentials because the results in the negative voltage range, where such a second component would make no contribution, allow close prediction of the Q vs. V behavior at positive potentials, where the second component comprised at least about one-third of Q_{ON} (squares or triangles in Fig. 3A).

In the course of these and other (Dubois and Schneider, 1981) studies, Q_{ON} vs. V data were obtained from nine fibers at 7.5–13°C. The parameter values and their standard errors obtained from the fit of Eq. 3 to the pooled data were -33.1 ± 1.0 mV for $\bar{V}$ and 13.3 ± 0.9 mV for k. The relative standard error in Q_{max} was $\pm 2.0\%$. The mean $\pm$ SEM of the parameter values obtained from fits to data from individual fibers were -32.1 ± 2.0 mV for $\bar{V}$ and 13.0 ± 0.9 mV for k. Our Q_{ON} results thus agree closely with those of Nonner et al. (1975), who obtained -33.7 mV for $\bar{V}$ and 14.9 mV for k in frog node of Ranvier.

Kinetics of ON and OFF Charge Movement at the Same Potential

The results in Figs. 2 and 3 indicate the presence of multiple components of gating charge movement at all potentials, even though the components may not always be separable kinetically. If, on the contrary, all charge movement were generated by a system having only a single voltage- and time-dependent transition, then at any given potential the ON and OFF charge movements should have the same time constants (e.g., Hodgkin and Huxley, 1952). We therefore examined ON and OFF Q time courses at the same potential to see whether such data could rule out the possibility of a single transition system. Fig. 4A presents records from one such experiment. The right-hand traces in each panel give the Q time courses for the voltage step sequences shown diagrammatically on the left. The ON charge movement at -30 mV (record *b*) was considerably slower than the OFF at the same potential (record *a*), which was recorded after first having moved the charge in the ON direction by a 200-μs prepulse to +20 mV. Semilog plots of ON and OFF charge movements at -30 mV, each obtained by averaging measurements from tracings of four records such as those in Fig. 4A, are presented in Fig. 4B. Both ON and OFF charge movements closely followed single exponentials, with time constants τ_{ON} of 250 μs and τ_{OFF} of 62 μs. Single exponential fits to the individual traces that were used for Fig. 4B gave τ_{ON} values ranging from 216 to 277 μs (mean $\pm$ SE = 250 ± 14 μs) and τ_{OFF} values from 50 to 79 μs (61 ± 7 μs).

ON and OFF charge movement time constants obtained at the same potential in each of several fibers are presented in Table II. For the potentials tested, which were all in the neighborhood of $\bar{V}$ for these fibers, τ_{ON} was 1.21–4.17 times larger than τ_{OFF} (mean $\pm$ SE, 2.52 ± 0.29). Such a discrepancy between ON and OFF time constants is incompatible with a system having only a single-voltage and time-dependent transition, even though a single exponential does provide a good description of these ON and OFF charge movement time courses.

The voltage dependencies of τ_{ON} and τ_{OFF} were also investigated. Results from one fiber are presented in Fig. 5. Over the voltage range where both time constants could be determined, τ_{ON} (filled circles) was two to three times larger than τ_{OFF} (open circles). Considering the scatter in the measurements, it is difficult to tell whether τ_{ON}/τ_{OFF} was constant or varied with the voltage.

Since τ_{OFF} was always measured after a 200-μs prepulse to positive potentials, it might be argued that the voltage dependence of the charge movement

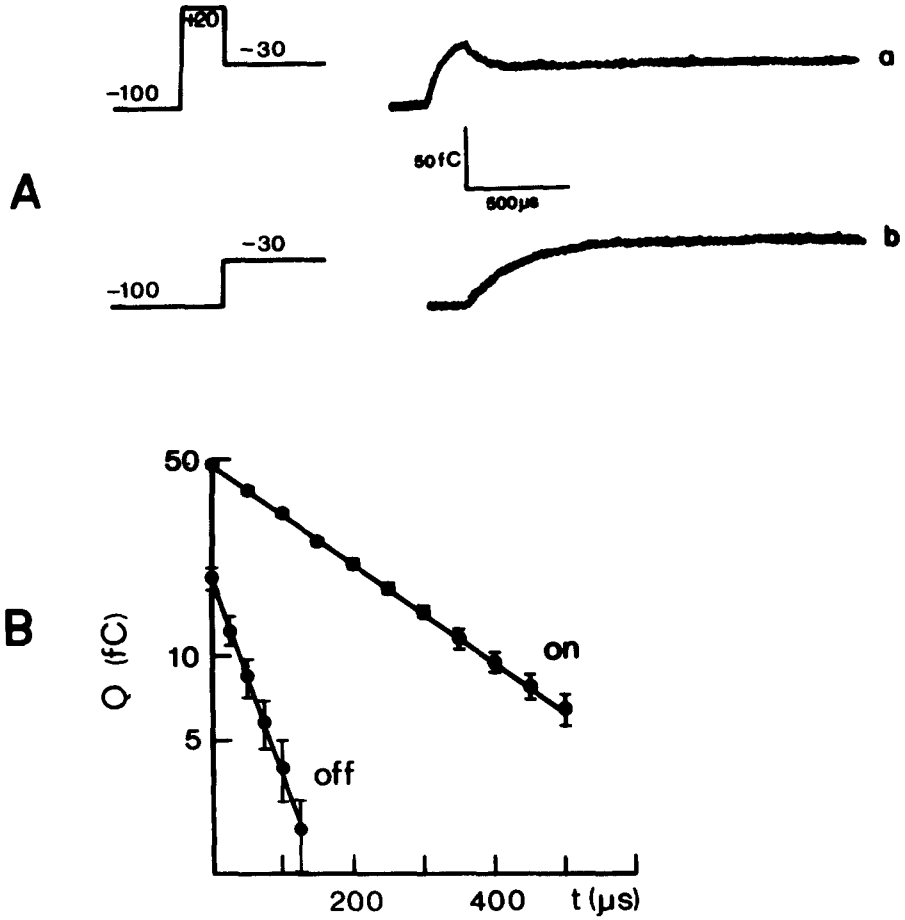

FIGURE 4. ON and and OFF charge movement kinetics at the same potential. (A) Traces of charge movement recorded during pulses to −30 mV applied either after 200 μs depolarizations to +20 mV (*a*, OFF response) or from the holding potential (*b*, ON response). Pulse programs shown on the left. (B) Semilogarithmic plot of average ON and OFF charge movements (four recordings of each) at −30 mV obtained using pulse programs shown in part A. The time constants for ON and OFF charge movements are, respectively, 250 and 62 μs. Temperature: 7.5°C. Fiber: 22-1-80.

process had been modified by the prepulse, as, for example, accompanying "charge immobilization" (Armstrong and Bezanilla, 1977; Nonner, 1980). Figs. 6A and B, which present the Q_{ON} and Q_{OFF} values corresponding to the τ_{ON} and τ_{OFF} data in Fig. 5, indicate that this was not the case. Both the charge Q_{ON} moved outward during a single step and the charge Q_{OFF} moved back after a 200-μs ON prepulse to +20 mV gave essentially identical values of $\bar{V}$ and k when fit by Eq. 3 or its complement for Q_{OFF}. The simplest interpretation of this result is that the relative energy levels of the various potential energy wells that the charges occupy in the membrane were not significantly altered by the prepulse.

The OFF value for Q_{max} obtained from the data in Fig. 6B was only 68% of the OFF value obtained from the data in Fig. 6A. At the prepulse voltage of

TABLE II

TIME CONSTANTS FOR ON AND OFF CHARGE MOVEMENTS AT THE SAME MEMBRANE POTENTIAL

Fiber	V	τ_{ON}	τ_{OFF}	τ_{ON}/τ_{OFF}
	mV	μs	μs	
3-1-80	−30	262	96	2.73
8-1-80	−40	103	85	1.21
8-1-80A	−40	248	155	1.60
16-1-80	−40	260	129	2.02
22-1-80	−30	250	60	4.17
30-1-80	−40	367	120	3.06
	−30	245	80	3.04
1-2-80	−30	268	103	2.60
	−40	269	121	2.22
Mean±SEM				2.52±0.29

OFF charge movements were recorded after 200-μs ON prepulses to +20 mV, whereas ON charge movements were recorded using pulses directly from the −100-mV holding potential.

+20 mV only 86% of the steady-state value of Q_{ON} was found to be moved during the first 200 μs of the prepulse. Since the fit of Eq. 3 to the steady-state Q_{ON} data indicated that at +20 mV Q_{ON} was 99% of Q_{max}, the OFF value for Q_{max} could be at most only 85% of the ON value. If the remaining deficit is attributed to charge immobilization, the percent of the 200-μs Q_{ON} that was not immobilized during the prepulse was 80% [= 100(0.68/0.85)].

For a single energy barrier located between two possible sites that the intramembrane charged particles can occupy, the time constant vs. voltage relationships shown in Fig. 5 should be described by the equation

$$\tau = 2\tau_{\bar{V}}/\{\exp[\eta(V - \bar{V})/k] + \exp[(1 - \eta)(\bar{V} - V)/k]\} \quad (4)$$

(Adrian, 1978; Horowicz and Schneider, 1981*b*), where $\tau_{\bar{V}}$ is the value of τ at $\bar{V}$ and η is the fraction of the total field between sites that appears between the barrier peak and the resting site. Values of the parameters $\bar{V}$ and k in Eq.

4 were determined from the fits to the charge vs. voltage relationships presented in Fig. 6. Assuming the barrier to be symmetrically positioned between the two sites, η is 1/2 and $\tau\bar{v}$ is the maximum value τ_{max} of τ (Keynes and Rojas, 1974). For this case the value of τ_{max} was adjusted to give the best fits to either the τ_{ON} or τ_{OFF} data. One may observe that the resulting theoretical curves (solid in Fig. 5) poorly describe the experimentally determined τ-V relationships. The τ_{OFF} values are in rough agreement with the

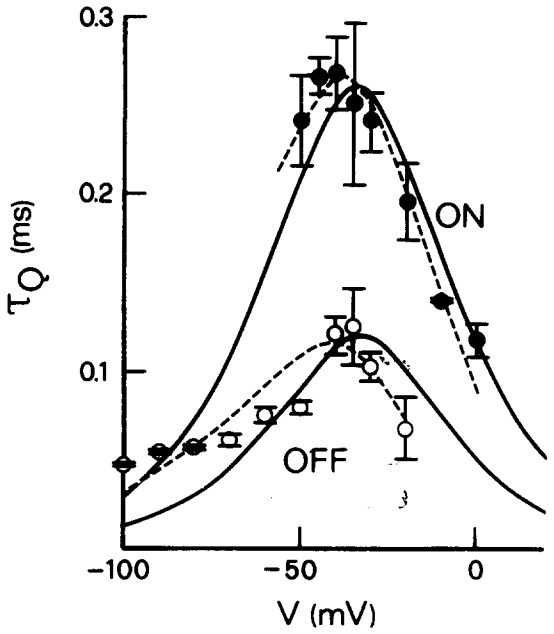

FIGURE 5. ON and OFF time constant vs. voltage relationships. The ON charge movement was recorded during pulses of various amplitudes applied from the holding potential. The OFF charge movement was recorded during pulses of various amplitudes preceded by 200-μs depolarizations to +20 mV. Mean values and standard errors of two to nine determinations. The curves are drawn according to Eq. 4 using the values of $\bar{V}$ and k determined from the fits to the charge vs. voltage relationships presented in Fig. 6. For the solid curves η = 0.500 and $\tau\bar{v}$ = 260 μs (ON) and 120μs (OFF). For the dashed curves, η = 0.604 (ON) and 0.690 (OFF) and $\tau\bar{v}$ = 261 μs (ON) and 107 μs (OFF). Temperature: 8°C. Fiber: 1-2-80.

theoretical τ_{OFF}-V curve over a voltage range positive to about −60 mV, but at the most negative potentials they are closer to the theoretical curve for τ_{ON} than to that for τ_{OFF}. This may explain why previous determinations of τ_{ON} and τ_{OFF} over non-overlapping voltage ranges were thought to follow a single τ vs. V relationship (Keynes and Rojas, 1974). Allowing the barrier to be asymmetrically located and using a linearized form of Eq. 4 to determine η

and $\tau\bar{v}$ (Horowicz and Schneider, 1981*b*) gave the dashed theoretical curves, which correspond more closely to the data in Fig. 5.

Effect of ON *Pulse Duration on* OFF *Charge Movement*

Using a holding potential at the negative end of the Q vs. V relationship, Q_{ON} is measured using a single pulse, whereas Q_{OFF} must be measured after a prepulse that moves some or all charge in the ON direction. It has been reported that τ_{OFF} at a given potential depends on the duration of the preceeding pulse (Armstrong and Bezanilla, 1977; Nonner et al., 1978). In view of our observation that ON and OFF Q time constants are not equal at the same potential, we reinvestigated the effect of the ON prepulse duration on OFF charge movement.

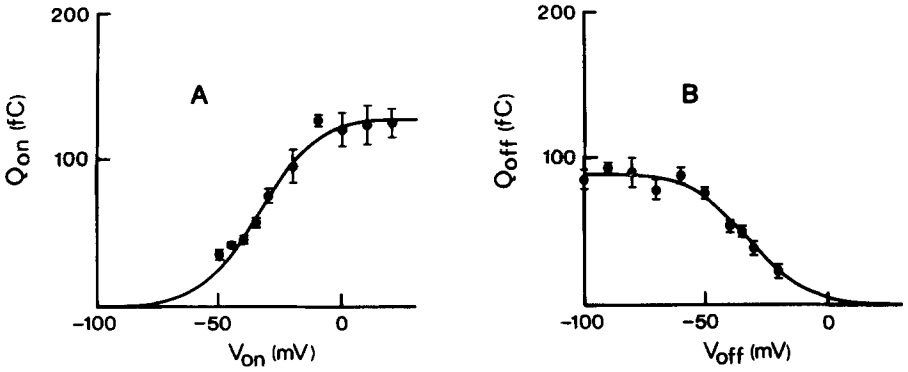

FIGURE 6. ON and OFF charge movement vs. voltage relationships. (A) ON charge movement recorded during pulses to various potentials applied from the holding potential. (B) OFF charge movement recorded during pulses to various potentials preceded by 200-μs depolarizations to +20 mV. Mean values and standard errors of two to six determinations. The curves are nonlinear least-squares fit of Eq. 3. The values of the parameters Q_{max}, $\bar{V}$, and k and their standard errors are, respectively: 130 ± 6 *fC*, −33.7 ± 1.7 mV, and 11.6 ± 2.1 mV (ON response), and 89 ± 3 fC, −33.1 ± 1.8 mV, and 11.0 ± 2.4 mV (OFF response). Same fiber and run as for Fig. 5.

Two parameters of charge movement are known to change with time during relatively large depolarizing pulses: Q_{ON} increases with time to its final value and charge immobilization develops (Armstrong and Bezanilla, 1977; Nonner, 1980). Fig. 7 presents the time course of charge immobilization. Q_{OFF} was monitored at −80 mV after ON pulse durations of up to 3 ms at +20 mV and normalized to the final value $Q_{ON\infty}$ of Q_{ON} at +20 mV in each of four fibers. The time course of normalized Q_{OFF} in Fig. 7 was described by the equation

$$\frac{Q_{OFF}}{Q_{ON\infty}} = \frac{Q_{ON}}{Q_{ON\infty}}\left[\frac{Q_{OFF\infty}}{Q_{ON\infty}} + \left(1 - \frac{Q_{OFF\infty}}{Q_{ON\infty}}\right)e^{-t_{ON}/\tau_i}\right], \quad (5)$$

where Q_{ON} and Q_{OFF} are both functions of the ON pulse duration t_{ON}, $Q_{OFF\infty}$/

$Q_{ON\infty}$ represents the immobilization-resistant fraction of charges, and τ_i is the immobilization time constant. In agreement with the observations of Armstrong and Bezanilla (1977) and Nonner (1980), $Q_{OFF\infty}/Q_{ON\infty} = 0.33$. Also in agreement with Nonner (1980), the value of τ_i used in the fit of Fig. 7 was 800 μs, somewhat larger than the mean value of the fast inactivation time constant for I_{Na} of 480 ± 21 μs determined in the same fibers at the same ON potential of +20 mV.

The influence of ON pulse duration on the kinetics of Q_{OFF} are considered in Fig. 8. Part A presents semilog plots of Q_{OFF} at −80 mV in one fiber after pulses of 100 (*a*), 600 (*b*), and 2,000 μs (*c*) to +20 mV. The three time courses

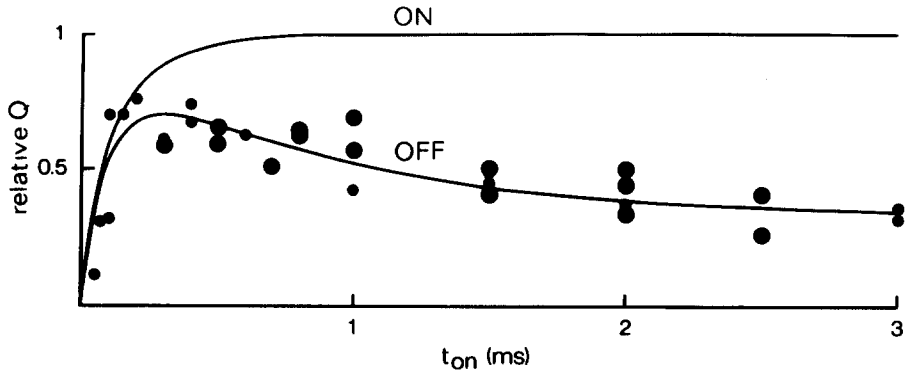

FIGURE 7. Immobilization of charge movement. Q_{ON} at +20 mV and Q_{OFF} at −80 mV were determined on four fibers for different ON pulse durations t_{ON} at +20 mV and were normalized to the average steady state Q_{ON} in the same fiber at +20 mV. The line for relative Q_{ON} was drawn through the average values of normalized Q_{ON} determined every 100 μs (two to six determinations for each fiber.) Q_{OFF} values were generally determined several times on each fiber. The smallest points denote single determinations, the medium points denote averages of two or three determinations, and the largest points denote averages of four to six determinations, each for a given fiber at a given ON duration. The line through the relative Q_{OFF} values was drawn according to Eq. 5 with $Q_{OFF\infty}/Q_{ON\infty} = 0.33$ and $\tau_i = 800$ μs. Temperature: 8–8.5°C. Fibers: 21-2-80 A, 18-4-80, 25-4-80, 28-4-80.

are all quite well described by a single exponential, as was the case in other experiments. τ_{OFF} after the 600-μs pulse was larger than τ_{OFF} after either the 100- or 2,000-μs pulses. Fig. 8B presents τ_{OFF} at −80 mV as a function of the duration t_{ON} of the preceding pulse at +20 mV. τ_{OFF} first increased with increasing t_{ON}; then for t_{ON} values greater than ~600–1,000 μs, τ_{OFF} decreased with increasing t_{ON}.

It is tempting to relate the initial rise in τ_{OFF} to increasing Q_{ON} and to relate the later decline in τ_{OFF} to charge immobilization, which has been shown to be accompanied by increased speed of movement of the remaining nonimmobilized charge (Nonner, 1980). Fig. 8C presents Q_{ON} at +20 mV and Q_{OFF}

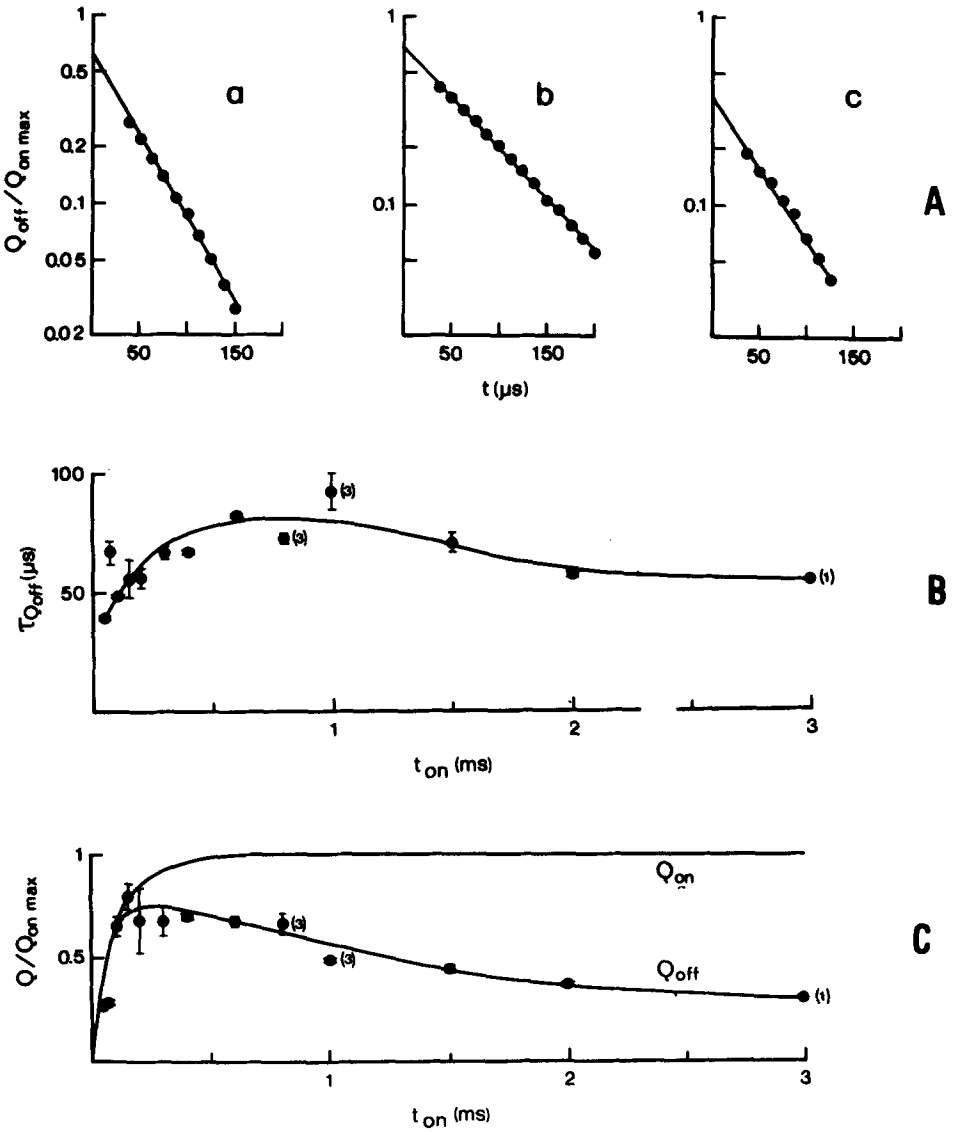

FIGURE 8. Effect of ON pulse duration on OFF charge movement kinetics. (A) Semilogarithmic plots of Q_{OFF} at −80 mV after ON pulses of 100 (*a*), 600 (*b*), and 2,000 μs (*c*) at +20 mV. (B) OFF time constant at −80 mV as a function of the duration of the ON prepulse at +20 mV. (C) Q_{ON} at +20 mV and Q_{OFF} at −80 mV relative to $Q_{ON\ max}$ as a function of the duration of the ON prepulses to +20 mV. In B and C most of the points are mean values of two determinations. Numbers of determinations differing from two appear in brackets. Curves were drawn by eye. Temperature: 8.5°C. Fiber: 21-2-80 A.

at −80 mV, both as a function of t_{ON} at +20 mV. The late declining phase of Q_{OFF} does indeed seem to parallel the late decline in τ_{OFF}. However, the early rise of Q_{ON} is relatively more rapid than the more prolonged early rising phase of τ_{OFF}.

The relationship between ON charge movement and the increasing phase of τ_{OFF} is further explored in Fig. 9, which presents τ_{OFF} as a function of $Q_{ON}/$

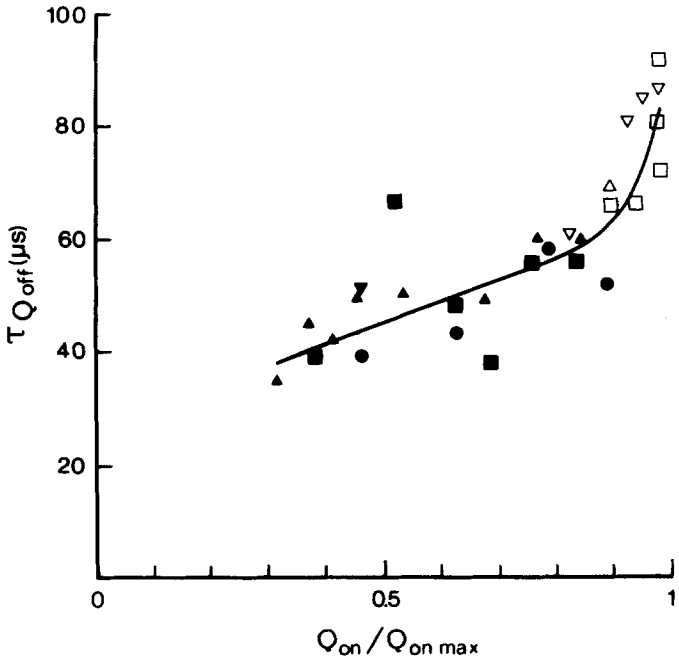

FIGURE 9. OFF charge movement time constant as a function of the relative quantity of charge moved during the preceding ON pulse. τ_{OFF} was measured in four fibers (different symbols) at −80 mV after ON prespulses of varying duration at either 0 or +20 mV. The filled symbols give results for $t_{ON} \leq 300$ μs at 0 mV or ≤200 μs at +20 mV. The open symbols are for longer t_{ON} values for which τ_{OFF} is probably underestimated because of the onset of charge immobilization. Q_{ONmax} for each fiber was calculated from the steady value of Q_{ON} at 0 or +20 mV in the same fiber using Eq. 3 with $\bar{V} = -33.1$ mV and $k = 13.3$ mV. Curve was drawn by eye. Temperature: 7–10°C. Fibers: 21-2-80 A (■), 22-2-80 (●), 7-3-80 (▲), and 28-4-80 (▼).

Q_{max} for the experiment of Fig. 8 and for three other experiments in which τ_{OFF} was measured at −80 mV after ON prepulses of varying duration at either 0 or +20 mV. The filled symbols give results for $t_{ON} \leq 300$ μs at 0 mV or for $t_{ON} \leq 200$ μs at +20 mV. Open symbols are for longer t_{ON} values at the same potentials. They include results for ON durations up to and including those giving the maximum τ_{OFF}. The increase of τ_{OFF} with Q_{ON} occurs over the

entire range of Q_{ON}/Q_{max} studied, but is clearly most marked as Q_{ON} nears Q_{max}. In fact, the pronounced increase in τ_{OFF} with movement of the last part of Q_{ON} was probably even more striking than Fig. 9 indicates because for the open symbols τ_{OFF} was most likely underestimated to an unknown extent by the onset of charge immobilization. If all of the increase in τ_{OFF} were a direct consequence of ON charge movement, the last 5–10% of Q_{ON} must clearly have a much more marked effect on τ_{OFF} than the preceeding 90–95%. Alternatively, if two different processes were involved, one process might be directly related to the amount of ON charge movement and might give rise to the gradual phase of increasing τ_{OFF} with Q_{ON}/Q_{max}. A second parallel voltage- and time-dependent process, which is independent of the amount of charge moved but which alters the rate of charge movement and sets in more slowly than ON charge movement, might give rise to the apparent steep phase of increasing τ_{OFF} with the last 5–10% of Q_{ON}/Q_{max} (see Discussion).

ON and OFF Charge Movement Kinetics in the Absence of Charge Immobilization

The increase in τ_{OFF} with ON pulse duration was apparently normally obscured by the onset of effects most likely associated with I_{Na} inactivation and charge immobilization. It was therefore of interest to study τ_{OFF} in the absence of the inactivation process. Since iodate has been shown to remove I_{Na} inactivation (Stämpfli, 1974), its effect on charge movement was investigated. Fig. 10 presents results from an experiment in which ON and OFF charge movements were monitored before and after changing the cut end solution to one in which 30 mM $NaIO_3$ replaced an equimolar amount of CsCl in the normal cut end solution. Traces on the left were obtained under control conditions and those on the right were recorded 14–24 min after changing the cut end pools to the IO_3^- solution. The upper traces indicate that IO_3^- treatment almost completely eliminated charge immobilization. For 1.5-ms pulses from −100 to 0 mV, the ratio of mean Q_{OFF} to mean Q_{ON} was 0.58 for five control traces and 0.99 for three traces after IO_3^- treatment. IO_3^- also decreased the mean value of Q_{ON} for these pulses to 59% of the control value, which is indicative of general fiber deterioration. In fact, the fibers were quite unstable once iodate became effective, and many Q records had to be discarded because of obvious changes in leakage current during the summing process or even during individual pulses. This made the iodate effect quite difficult to study and only two experiments were successful. The iodate treatment was, however, preferable to the use of either sea anemone (*Anemonia sulcata*) or scorpion (*Androctonus australis Hector*) toxins, which slow but do not eliminate I_{Na} inactivation (Bergman et al., 1976; Romey et al., 1976; Bernard et al., 1977; unpublished personal observations).

The effect of internal IO_3^- on ON and OFF charge movement time courses at −30 mV is shown by traces *b* and *c* in Fig. 10. The ON time course was little affected by iodate, whereas the OFF was considerably slowed. This is shown more clearly in Fig. 11, which presents semilog plots of normalized average values obtained from two or three traces as in Fig. 10*b* or *c*. At −30 mV, τ_{ON} was 246 μs in control and 245 μs after iodate, whereas τ_{OFF} increased from 83 to 269 μs after iodate treatment. The interesting finding that after iodate

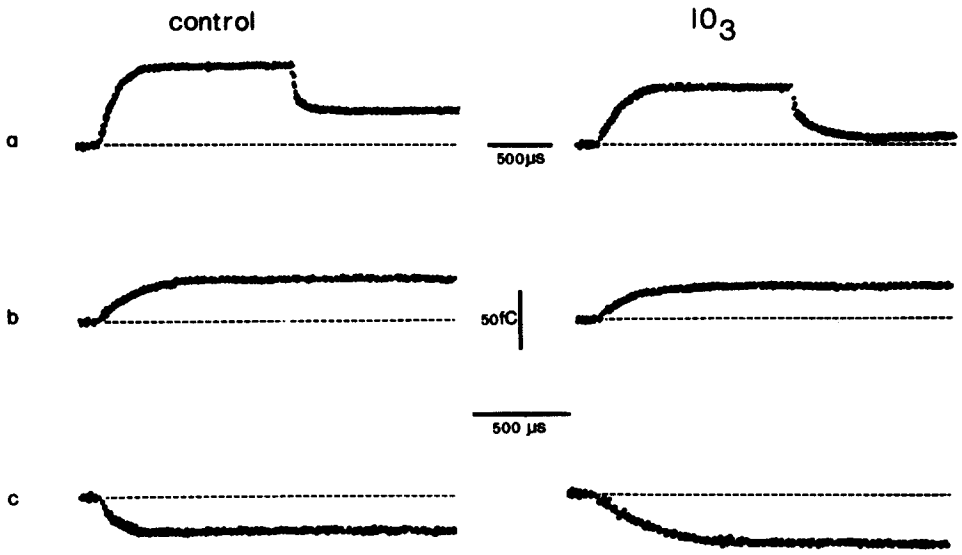

FIGURE 10. Effects of internal iodate on charge movement. The charge movement was recorded during and after pulses to 0 mV applied from the holding potential (*a*, ON and OFF responses), during pulses to −30 mV applied from the holding potential (*b*, ON response) and during pulses to −30 mV applied after 1,500-μs depolarizations to 0 mV (*c*, OFF response) in control conditions (left) and 14–24 min after replacing 30 mM CsCl by 30 mM $NaIO_3$ in the side pools' solution. In the presence of IO_3, the charge immobilization was almost eliminated and the OFF charge movement was slowed down. Temperature: 13°C. Fiber: 5-6-80 A.

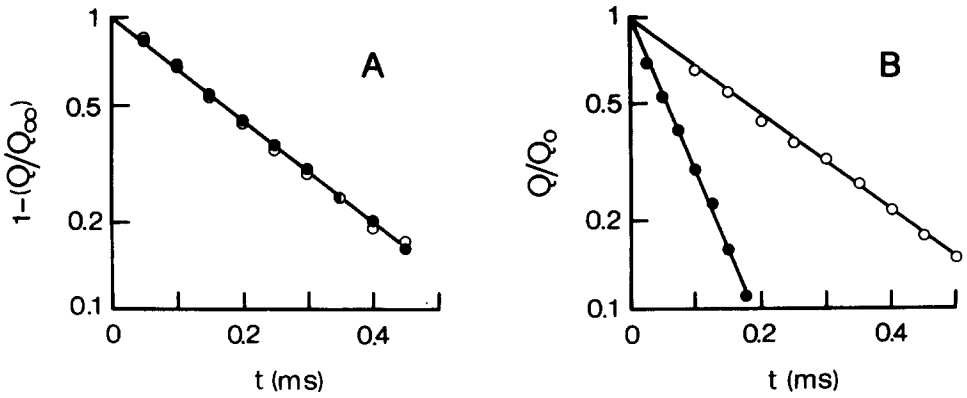

FIGURE 11. Semilogarithmic plots of ON (A) and OFF (B) charge movements at −30 mV in control conditions (filled circles) and during diffusion of iodate in the axoplasm (open circles). The OFF charge movement was recorded after 1,500-μs prepulses to 0 mV. The points are average values obtained from two or three traces. In control and iodate, respectively, τ_{ON} is 246 and 245 μs, τ_{OFF} is 83 and 269 μs. Temperature: 13°C. Fiber: 5-6-80 A.

treatment τ_{OFF} following a relatively long ON prepulse became equal to τ_{ON} at the same potential was confirmed in the one other fiber in which the iodate effect was successfully studied. Fiber instability unfortunately prevented determination of the voltage and time dependencies of τ_{ON} and τ_{OFF} with charge immobilization eliminated by iodate.

OFF *Time Course of Sodium Current*

Data regarding the relative kinetics of charge movement and sodium conductance may prove to be important for distinguishing between alternative models for sodium channel gating. We have therefore re-examined the relationship between the OFF kinetics of I_{Na} and Q, devoting special attention to the effects of ON pulse duration.

In five out of a total of seven fibers in which the OFF time courses of I_{Na} and Q were both successfully monitored, the I_{Na} tails were completely characterized by a single exponentially decaying component. Sodium tail currents obtained from one such fiber are presented in part A of Fig. 12, which gives I_{Na} at OFF potentials of −100, −80, and −60 mV after 300-μs pulses to +20 mV. Semilog plots (part B) of values measured from tracings of the records in part A show that these I_{Na} tails followed single exponential time courses from 37.5 μs after pulse OFF at −100 or −80 mV and from 50 μs after pulse OFF at −60 mV. For comparison, records and semilog plots of Q_{OFF} obtained for the same pulses in the same fiber after the addition of TTX are presented as parts C and D of Fig. 12. Q_{OFF} was well described by a single exponentially decaying component from 12.5 μs after pulse OFF at each OFF voltage. In the two fibers in which I_{Na} tails did not follow a single exponential decay, a second smaller and slower exponentially decaying component was also present (see also Neumcke et al., 1976; Goldman and Hanin, 1978). In these two fibers the slower I_{Na} component had a time constant 3.2 or 3.1 times that of the faster component and, based on extrapolation to the start of pulse OFF, comprised only 3.9 or 9.5% of the initial OFF amplitude of I_{Na}. Only the time constant of the faster component of I_{Na} was used for comparison with Q_{OFF}. Since the remainder of the results deal exclusively with OFF time constants for I_{Na} and Q, these will simply be denoted here by τ_{Na} and τ_Q without any specific indication for pulse OFF.

Voltage Dependence of OFF *Time Constants for Sodium Current and Charge Movement*

Sodium current tails and OFF charge movements were recorded at several OFF membrane potentials in each of three fibers, giving the results in Fig. 13. In each fiber OFF pulses at various membrane potentials were preceded by a pulse of a set duration to a given positive potential. The OFF time constants τ_{Na} and τ_Q both tended to become smaller as the OFF voltage was made more negative. τ_Q was always equal to or slightly larger than τ_{NA}. No consistent effect of V_{OFF} on τ_Q/τ_{Na} is apparent in the data in Fig. 13. These results are different from those obtained by Neumcke et al. (1976), who found τ_Q/τ_{Na} to be ~3 for OFF

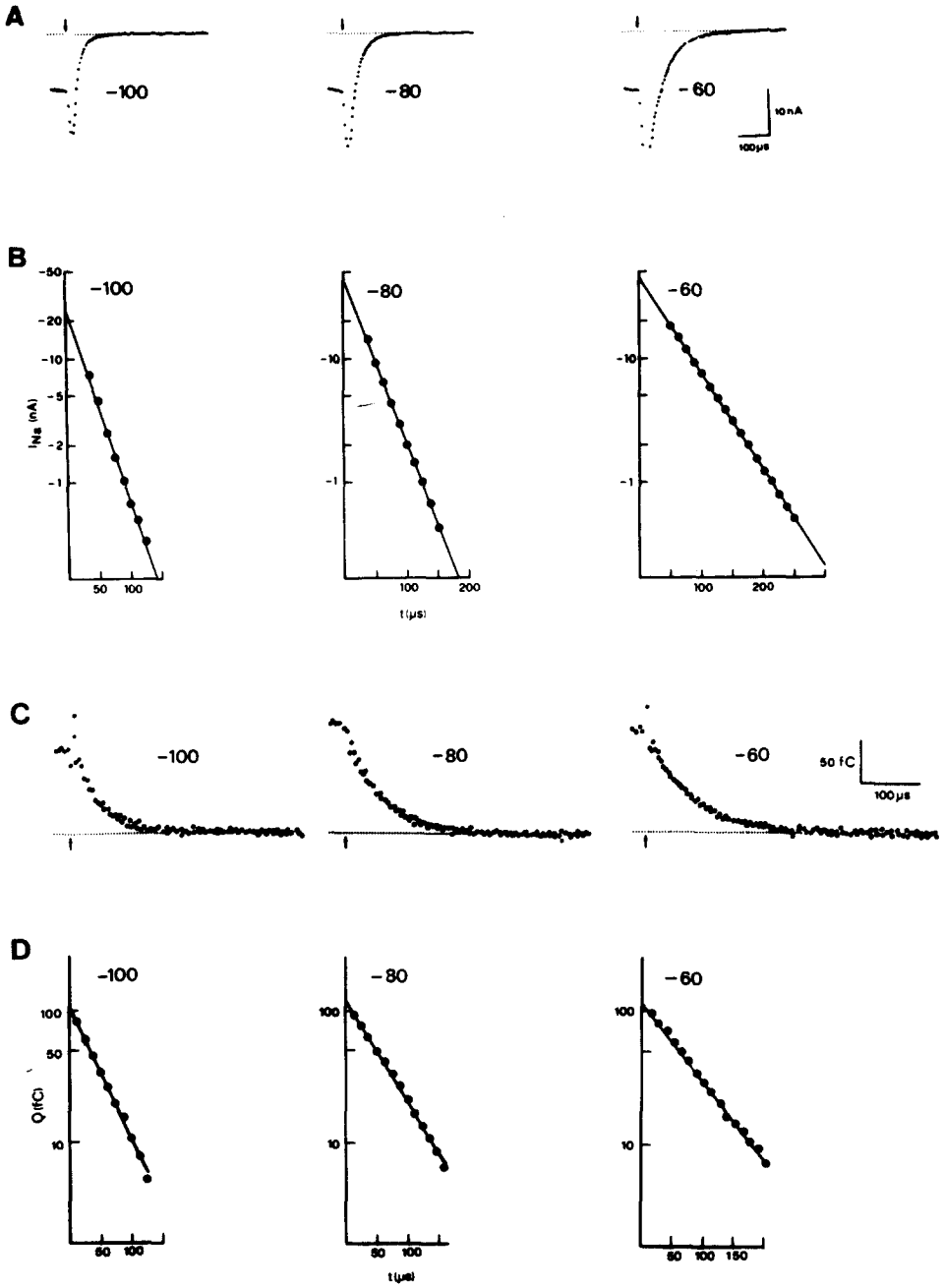

FIGURE 12. OFF time course of sodium current and charge movement. (A) Tails of sodium current recorded at different membrane potentials (−100, −80, −60 mV) after activation of the conductance by 300 μs depolarizations to +20 mV terminated at the arrows. (B) Semilogarithmic plots of values obtained from tracings of the records shown in part A. (C) OFF charge movement for the same pulses as in part A. The arrow marks pulse OFF; the four points before the arrow give final values of charge during the pulse. (D) Semilogarithmic plots of values obtained from tracings of the records in part C. Temperature: 8.5°C. Fiber: 20-2-80.

voltages near −100 mV in frog node of Ranvier under similar conditions. The source of this discrepancy is not clear (see Discussion).

One possible problem with comparing time courses of I_{Na} and Q is that during large sodium currents, significant voltage drops may occur across any resistance in series with the membrane, causing differences between the

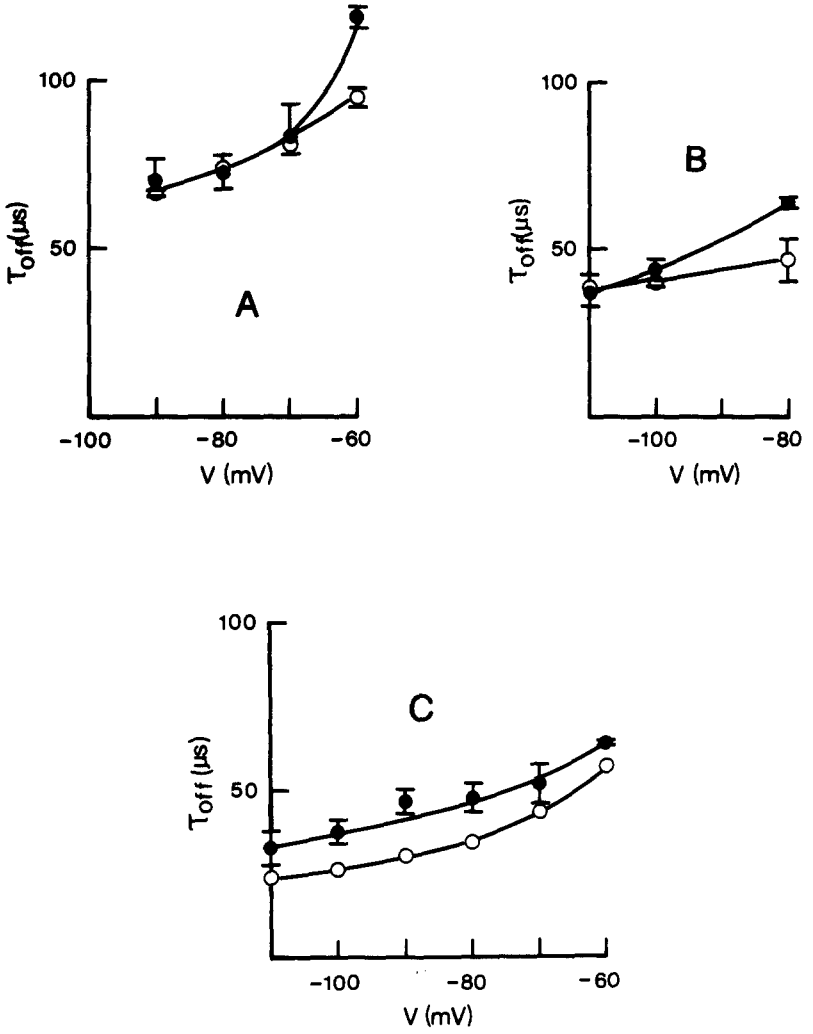

FIGURE 13. Voltage dependence of OFF time constants for sodium current and charge movement. OFF time constants for sodium current (open circles) and charge movement (filled circles) were determined on three different fibers (A, B, and C) during pulses to various potentials preceded by ON pulses to +30 mV for 200 μs (A) or to +20 mV for 300 μs (B and C). Mean values and standard errors of several determinations at each potential (three or four for Q, two or three for I_{Na}). Curves were drawn by eye. Temperature: 9.5°C (A), 9°C (B), 8.5°C (C). Fibers: 6-2-80 A (A), 21-2-80 (B), 20-2-80 (C).

apparent and true transmembrane potential (Drouin and Neumcke, 1974). Such series resistance artifacts should not pose any problem for gating charge measurements that involve only small currents. Fig. 14 presents a test for the effect of series resistance artifacts in measuring OFF time constants of I_{Na}. Sodium current tails were measured in the standard control solution and then in the same solution plus 4 nM TTX, which diminished I_{Na} to ~40% of control. Normalized semilog plots of Na tail currents at −70 mV in the two solutions are presented in part A of Fig. 14 and appear to be virtually identical. Part B of Fig. 14 presents the OFF voltage dependence of τ_{Na} obtained in the two solutions. At and negative to −70 mV the OFF time constants were the same for control and partially depressed sodium currents, indicating no significant effect of the series resistance artifact on the determination of τ_{Na}.

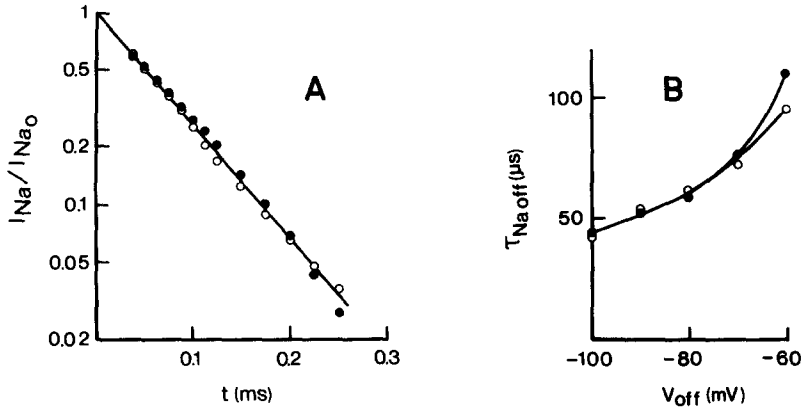

FIGURE 14. Test for series resistance artifact. Sodium tail currents were recorded in standard control solution (filled circles) and then in the same solution plus 4 nM TTX (open circles) during OFF pulses to various potentials preceded by ON depolarizations to 0 mV lasting 400 μs. (A) Semilogarithmic plot of normalized sodium tail currents recorded at −70 mV. (B) OFF time constants for I_{Na} as a function of OFF membrane potential. Curves were drawn by eye. Temperature: 8°C. Fiber: 25-2-80 A.

Effects of ON Pulse Duration on OFF Time Constants for Sodium Current and Charge Movement

Fig. 15 presents OFF time constants τ_Q and τ_{Na} at −80 mV as a function of the preceding ON prepulse duration t_{ON} at +20 mV. As in Fig. 8B, τ_Q first increased as t_{ON} was increased up to ~0.7 to 1 ms and then decreased for longer t_{ON}'s. In contrast, τ_{Na} increased with t_{ON} toward a maximum level, which then remained approximately constant for ON durations from ~1.5 to 2.5 ms. The monotonic rise in τ_{Na} with t_{ON} generally paralleled the rising phase of τ_Q. However, the declining phase of τ_Q at longer ON durations, which paralleled the fall in Q_{OFF} in this fiber as in the fiber shown in Fig. 8, was not reflected by a decline in τ_{Na}.

Mean normalized τ_{Na} values from the fiber in Fig. 15 and from two other fibers are presented in Fig. 16A, also as a function of prepulse t_{ON}. These data confirm that the sodium current OFF time constant at −80 mV exhibits no decline for ON pulse durations longer than 1 ms. Since τ_Q declines with the development of charge immobilization, whereas τ_{Na} does not, it must be concluded that this alteration in Q kinetics cannot be due to a nonspecific change in membrane properties but must be attributed specifically to the nonimmobilized gating charges of inactivated sodium channels.

The effect of t_{ON} on the ratio of OFF time constants τ_Q/τ_{Na} is examined for the same three fibers plus one other in Fig. 16B. For ON prepulse durations up to ~0.5 ms the ratio appeared to be almost independent of t_{ON}, supporting the parallel rising phase of τ_Q and τ_{Na} with t_{ON}. Then for pulses longer than

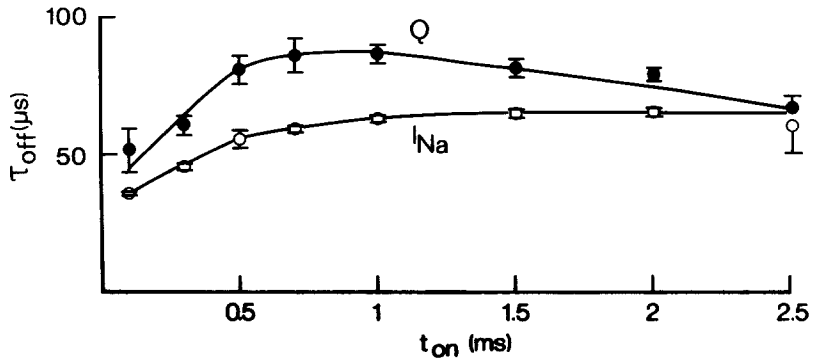

FIGURE 15. Effects of ON pulse duration on OFF time constants for sodium current and charge movement. OFF time constants for sodium current (open circles) and charge movement (filled circles) were determined at −80 mV after ON depolarizations of various durations (t_{ON}) at +20 mV. Mean values and standard errors of several determinations (three for τ_{Na}, two to five for τ_Q). Curves were drawn by eye. Temperature: 8°C. Fiber: 28-4-80.

~0.5 ms τ_Q/τ_{Na} decreased with increasing t_{ON} due to declining τ_Q and constant τ_{Na}.

To highlight trends in τ_Q/τ_{Na} as a function of t_{ON}, fiber to fiber variation in absolute levels of τ_Q/τ_{Na} were minimized by using the following normalization routine for Fig. 16B: the data from each fiber were scaled so that the mean of all values of τ_Q/τ_{Na} in that fiber for ON pulse durations between 100 and 500 μs was equal to the mean of the individual means from the four fibers for the same range of pulse durations.

All values of τ_Q/τ_{Na} obtained in these experiments for 200- or 300-μs pulses to +20 to +50 mV followed by OFF's at −70 to −90 mV are given in Table III. For such pulses, which should be little affected by the inactivation process, the OFF time constant for charge movement was ~20% larger than the time constant for decay of I_{Na}.

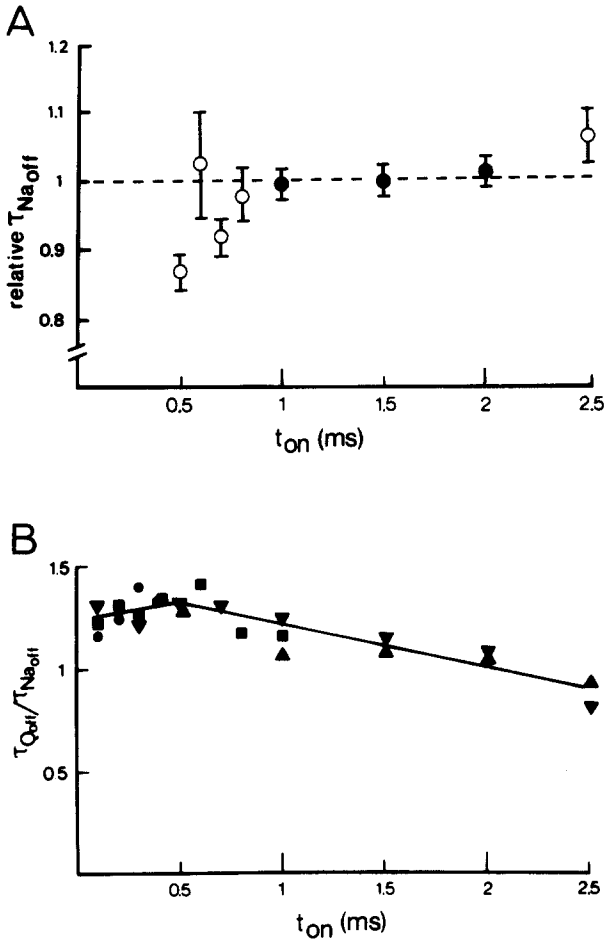

FIGURE 16. Effect of ON pulse duration on the OFF time constant for sodium current and on the ratio of OFF time constants τ_Q/τ_{Na}. (A) Sodium tail currents were recorded in three different fibers at −80 mV after ON depolarizations to +20 mV of various durations (t_{ON}). For each fiber, the OFF time constants were normalized to their mean values for t_{ON} between 1 and 2 ms (filled circles). Temperature: 8°C. Fibers: 18-2-80, 25-4-80, 28-4-80. (B) Sodium current and charge movement were recorded in four different fibers. For each fiber, the OFF time constants τ_Q and τ_{Na} were determined at the same potential (−80 to −60 mV) after depolarizations of various durations (t_{ON}) to constant voltage (+20 or +30 mV) and their ratio was calculated. Ratios from different fibers were normalized as described in the text. Curve was drawn by eye. Temperature: 8–9.5°C. Fibers: 6-2-80 (●), 18-2-80 (■), 25-4-80 (▲), 28-4-80 (▼).

DISCUSSION

Comparison with Previous Observations

Generalizing from studies on squid axons, almost all of the charge movement recorded from nerve fibers appears to be involved with gating sodium channels (Yeh and Armstrong, 1978; Cahalan and Almers, 1979; Almers, 1978). Any acceptable model for sodium channel gating should therefore be capable of reproducing all properties of both sodium currents and charge movements in nerve. In an effort to further define some of these properties, present observations will be compared with previously published results.

To our knowledge, the present data concerning ON and OFF charge movement time constants at the same potential are the first such results reported in the literature. In several previous studies τ_{OFF} was determined over a voltage range negative to about −50 to −70 mV, whereas τ_{ON} was determined at more positive voltages (Keynes and Rojas, 1974 and 1976; Bullock and Schauf, 1978). Considering the scatter in the data, a single bell-shaped τ vs. V relationship appeared to be in reasonable agreement with both the τ_{ON} and τ_{OFF} values in such data sets. However, the present determinations of τ_{ON} and τ_{OFF} over an overlapping voltage range clearly show that in node of Ranvier τ_{ON} and τ_{OFF} cannot be described by the same τ vs. V relationship.

TABLE III

RELATIVE OFF TIME CONSTANTS FOR CHARGE MOVEMENT AND SODIUM CURRENT

Fiber	V_{ON}	t_{ON}	V_{OFF}	τ_Q/τ_{Na}
	mV	*μs*	*mV*	
20-2-80	+20	300	−90	1.52
			−80	1.39
			−70	1.18
21-2-80	+20	300	−80	1.37
28-4-80	+20	300	−80	1.34
6-2-80A	+30	200	−90	1.05
			−80	0.98
			−70	1.03
18-2-80	+50	200	−70	0.99
		300	−70	0.95
Mean±SEM				1.18±0.07

A further complication with some of the previous τ vs. V results might also be noted here, namely that changes in the holding potential were used as the method for altering V_{OFF} (Keyes and Rojas, 1974 and 1976). Such a procedure will cause τ_{OFF} to vary due to the combined results of (*a*) a varying degree of partial inactivation of the sodium channel gating mechanism and (*b*) the direct effect of V_{OFF} on τ_{OFF}. Since τ_{OFF} decreases with increasing inactivation (Nonner, 1980 and above), the increase of τ_{OFF} with increasingly positive values of V_{OFF} observed in such cases must have been less steep than would have been observed under the condition of constant inactivation.

The effects of ON pulse duration and amplitude on the OFF time constants for charge movement have been noted or studied in a number of reports.

Using pulses producing relatively little inactivation, it has previously been observed that for given ON and OFF voltages, τ_{OFF} increases with ON pulse duration in both squid axons (Armstrong and Bezanilla, 1974 [Fig. 5], 1977; Keynes and Rojas, 1974) and node of Ranvier (Nonner et al., 1978). The fact that τ_{OFF} increases with V_{ON} for pulses of set duration has also been noted for both squid axons (Keynes and Rojas, 1974; Meves, 1974) and node of Ranvier (Nonner et al., 1978). Neither of these effects was detected in *Myxicola* axons (Schauf et al., 1977). The decline in τ_{OFF} with pulse durations that would have produced significantly increasing sodium inactivation has been previously observed in both squid axons (Fig. 2 of Armstrong and Bezanilla, 1977) and node of Ranvier (Nonner et al., 1978; Nonner, 1980), but not in *Myxicola* axons (Table I of Bullock and Schauf, 1979). These comparisons seem to indicate that the sodium channel gating processes may be similar in squid and frog axons, at least insofar as can be determined from gating charge movement measurements, but that both may differ from the gating process in *Myxicola* axons. Further comparisons of present with previous results will therefore be restricted to studies on squid or frog axons.

In the present experiments it was observed that for pulses giving relatively little sodium inactivation the mean (± SEM) ratio of OFF time constants τ_Q/τ_{Na} was 1.18 ± 0.07 for V_{OFF}'s between −70 and −90 mV. This is in excellent agreement with the values of 1.18 ± 0.04 and 1.22 ± 0.03 obtained by Bezanilla and Armstrong (1975*a*, Table I) and by Armstrong and Bezanilla (1977, Table IV) from squid axons at $V_{OFF} = -70$ mV. However, it is considerably less than the values of 2.55 ± 0.05, 2.32 ± 0.06, and 1.92 ± 0.15 obtained by Neumcke et al. (1976, Table III) from three frog nodes at OFF voltages of −90, −82, and −74 mV, respectively. Separate comparison of OFF time constants at voltages near −90 mV shows good agreement of the present τ_Q values with those reported by Neumcke et al. (1976), whereas the present τ_{Na} values tended to be two to three times larger than those of Neumcke et al. One difference in procedure that might be thought to account for the different τ_{Na} values is that the first OFF points used in the present I_{Na} tail analyses occurred 37.5 μs after pulse OFF, wheres Neumcke et al. used points starting 15 μs after the pulse. Fast components of I_{Na} resolved by Neumcke et al. might thus conceivably have been missed in the present analysis. However, the I_{Na} tail records presented by Neumcke et al. (1976, Figs. 4B and 5B) were well described by a single exponential component from 15 to 100 μs after pulse OFF so that sampling starting at 15 or 37.5 μs should have resulted in similar values for τ_{Na}. As a further indication that time resolution was probably not a limiting factor in the present experiments, τ_{Na} was determined to be 24 μs at −110 mV in one fiber, in which case τ_Q/τ_{Na} was still only 1.39 (Fig. 13C). Since Neumcke et al. (1976) used 50-ms prepulses to the same potential as V_{OFF}, their τ_Q values for the more positive V_{OFF} levels are probably underestimated due to the effect of inactivation. Correcting for this effect would tend to increase their τ_Q/τ_{Na} values at the more positive V_{OFF} levels so that the discrepancy between our τ_Q/τ_{Na} values and those of Neumcke et al. should probably apply to all OFF voltages. The source of this discrepancy is not

known. In the experiments of Armstrong and Bezanilla (1977), inactivation was negligible at the holding potential of −70 mV so that no correction need be applied to the τ_Q values reported by those authors.

The present observation that the ratio of OFF time constants τ_Q/τ_{Na} changes minimally with increasing ON pulse durations t_{ON} giving little sodium inactivation confirms the observations of Armstrong and Bezanilla (1977, Table IV). In both cases there was a considerable increase in the OFF time constants for both I_{Na} and Q with t_{ON}, but both increased in parallel so that their ratio remained about constant.

Kinetic Models for Sodium Channel Activation

Previous studies of sodium and gating currents have already indicated that models for Na channel activation based on multiple identical and independent gating particles per channel are inadequate (Armstrong and Bezanilla, 1974; Armstrong, 1978; Neumcke et al., 1976). Our observations of two components of Q_{ON}, of unequal ON and OFF time constants for Q at a given voltage, of OFF τ_Q values that depend on the preceding ON pulse duration and of OFF τ_Q/τ_{Na} ratios of ~1.2 are also all inconsistent with such models. Armstrong and Gilly (1979) have rcently proposed a simplified version of the Armstrong and Bezanilla (1977) sequential state scheme that accounts for two components of Q_{ON}, a rising phase in ON gating current and a delay in I_{Na} activation. However, our simulations with the model and parameter values given by Armstrong and Gilly (1979) indicate that the ratio of OFF time constants τ_Q/τ_{Na} predicted by their model at −70 mV following 200- to 1,000-μs pulses to +50 mV varies from 0.30 to 1.13, respectively, due to increasing τ_Q and constant τ_{Na}. The Armstrong-Gilly scheme thus does not appear to account for the observed approximately constant τ_Q/τ_{Na} of ~1.2 found by Armstrong and Bezanilla (1977, Table IV) and ourselves.

The observed similarity of OFF time constants for I_{Na} and Q was one of the first indications that the unmodified Hodgkin-Huxley (1952) formalism could not account for both I_{Na} and Q (Armstrong and Bezanilla, 1974). It was suggested originally that this observation might be accounted for on the basis of a closed-loop scheme whereby channel deactivation proceeded by a path different from channel activation (Bezanilla and Armstrong, 1975*a* and *b*). However, Oxford (1981) recently demonstrated that a separate deactivation path is inconsistent with I_{Na} time courses during multiple step pulses, and Armstrong and Bezanilla (1977) and Armstrong and Gilly (1979) eliminated the separate deactivation path from their models.

Several relatively simple modifications of independent particle models can give rise to similar OFF time constants for I_{Na} and Q. Consider the model in which channel opening requires movement of three identical changed gating particles associated with the channel, with the rate constants for movement of each particle being voltage dependent but independent of the location of the other particles. This model, which corresponds exactly to the Hodgkin-Huxley (1952) equations for Na channel activation, is represented by the upper line

in the kinetic scheme A (Armstrong and Bezanilla, 1974)

$$\begin{array}{ccccccc} & & 3\alpha & & 2\alpha & & \alpha \\ X_4 & \rightleftharpoons & X_3 & \rightleftharpoons & X_2 & \rightleftharpoons & X_1 \\ & & \beta & & 2\beta & & 3\beta \\ & & & & & & \gamma_1 \uparrow\downarrow \delta_1 \\ & & & & & & X_1T \end{array} \qquad \text{(A)}$$

In this case X_1 is the conducting state and each transition contributes an equal amount of charge movement.

Now assume that once all three of the gating particles have crossed the membrane they can form a trimer X_1T that cannot cross the membrane. Such trimer formation by the X_1 to X_1T transition is represented perpendicular to the other transitions in scheme A to emphasize that it involves no charge movement but only interactions of charges that have already moved from their resting locations. In contrast to the other rate constants, γ_1 and δ_1 would thus be independent of potential. If only X_1T were conducting, trimer formation would constitute opening of the channel; if both X_1 and X_1T were conducting, trimer formation would promote the open condition. Scheme A constitutes a greatly simplified version of a recent model involving four gating particles with dimer, trimer, and tetramer formation after the individual particles cross the membrane (Baumann and Easton, 1981).

If it is assumed that γ and δ are both large compared with α and β, X_1 and X_1T would be in equilibrium so that $X_1/X_1T = \delta/\gamma$. Scheme A could then be reduced to an equivalent four-state scheme under appropriate adjustment of the rate constants for the transition from X_1 to X_2. Setting $f_1 = X_1/(X_1 + X_1T)$ in scheme A, one obtains

$$\begin{array}{ccccccc} & & 3\alpha & & 2\alpha & & \alpha \\ X_4 & \rightleftharpoons & X_3 & \rightleftharpoons & X_2 & \rightleftharpoons & X_1'. \\ & & \beta & & 2\beta & & 3f_1\beta \end{array} \qquad \text{(B)}$$

X_1' of scheme B equals $X_1 + X_1T$ of scheme A. The fraction of conducting channels would be $(1 - f_1)X_1'$ or X_1', depending on whether only X_1T or both X_1 and X_1T were conducting.

Scheme B with $f = 0.5$ has been used to simulate OFF I_{Na} and Q records at a potential where $\beta = 20$ ms^{-1} and $\alpha = 1$ ms^{-1} after ON responses of various durations at a potential where $\alpha/\beta = 10$. Using single exponential fits starting 30 μs after the start of the simulated records, the ratio of OFF time constants τ_Q/τ_{Na} ranged from 1.3 to 1.7 for Q_{ON}/Q_{max} values ranging from 0.38 to 0.95, respectively. These values seem acceptably close to those in Fig. 16B because inactivation, which would tend to decrease τ_Q but not τ_{Na} for the larger Q_{ON}/Q_{max} values (Figs. 15 and 16A), has not been considered in the simulation.

The presence of two components of ON charge movement for relatively large depolarizations (Figs. 2 and 3 and Table I) is not predicted by scheme B. This can be simulated while maintaining similar OFF τ_Q and τ_{Na} values by an alternative particle interaction step. Assume that once two of the three identical particles have crossed the membrane independently, they must form

a dimer before the third particle can cross. This is diagrammed in scheme C.

$$\begin{array}{ccccc} & & \overset{3\alpha}{\rightleftharpoons} & \overset{2\alpha}{\rightleftharpoons} & \\ X_4 & & X_3 & & X_2 \\ & & \underset{\beta}{\rightleftharpoons} & \underset{2\beta}{\rightleftharpoons} & \\ & & & \gamma_2 \uparrow\downarrow \delta_2 & \\ & & & \overset{\alpha}{\rightleftharpoons} & \\ & & & X_2D & X_1 \\ & & & \underset{\beta}{\rightleftharpoons} & \end{array} \qquad \text{(C)}$$

Assuming the dimerization step to be sufficiently rapid so as to always be at equilibrium, scheme C can be reduced to scheme D.

$$X_4 \underset{\beta}{\overset{3\alpha}{\rightleftharpoons}} X_3 \underset{2\beta f_2}{\overset{2\alpha}{\rightleftharpoons}} X_2' \underset{\beta}{\overset{\alpha(1-f_2)}{\rightleftharpoons}} X_1. \qquad \text{(D)}$$

Here $f_2 = X_2/(X_2 + X_2D)$ and $X_2' = X_2 + X_2D$. Simulations with scheme D with $f_2 = \frac{2}{3}$, $\alpha_{ON}/\beta_{ON} = 20$, OFF = 20 ms^{-1}, and $\alpha_{OFF} = 1$ ms^{-1} gave OFF τ_Q/τ_{Na} values of 1.0–1.6 for Q_{ON}/Q_{max} values of 0.43–0.95, again acceptably close to those observed. Q_{ON} records were also simulated with scheme D with $f_2 = \frac{2}{3}$. For α_{ON}/β_{ON} values giving Q_{ON}/Q_{max} greater than about 0.7, such simulated Q_{ON} records were resolvable into two exponential components with the slower component carrying 46–63% of the total Q_{ON}. For α_{ON}/β_{ON} values giving Q_{ON}/Q_{max} less than about 0.7, the simulated Q_{ON} records were well described by single exponentials.

Both schemes B and D can likely provide good approximations to the general time course of I_{Na} because it has already been shown that I_{Na} can be closely reproduced using a wide variety of relative values both for individual forward rate constants and for individual reverse rate constants in the four-state model (Bezanilla and Armstrong, 1975*b*). Although neither scheme predicts a voltage-dependent delay before the start of m^a activation kinetics (Neumcke et al., 1976) nor a rising phase in ON gating current (Armstrong and Gilly, 1979), both observations might be accounted for by including formation of the trimer X_4T from the state X_4, where all charges are in their resting location. With rapid equilibration, this trimerization reaction would result in reducing the effective rate constants for the X_4' to X_3 transition from 3α to $3\alpha f_4$ in schemes B or D. X_4' and f_4 would be analogous to X_1' and f_1.

The inequality of τ_{ON} and τ_{OFF} at a given voltage and the steep variation of OFF time constants for Q with movement of the last 5–10% of Q_{ON} are not predicted by schemes B or D. These observations might perhaps be explained on the basis of state Y beyond X_1 and states X_5 and X_6 before X_4 (Armstrong and Bezanilla, 1977; Armstrong and Gilly, 1979). Alternatively, they might both be due to changes in apparent rate constants for transitions between states. Such changes might develop and/or decay with time after a step change in voltage. If for each transition the fractional change in forward and reverse rate constants were the same, the steady charge vs. voltage relationship would not be altered. This would be in agreement with the similar observed Q vs. V relationships but different time constants for Q_{ON} and Q_{OFF}. In terms

of Eyring rate theory, identical fractional changes in forward and reverse rate constants would correspond to identical changes in energy barrier heights both for forward and reverse transitions. Starting from the general representation of any linear sequential model given by the upper line of scheme E (cf. Armstrong, 1978), a kinetic representation of this type of mechanism would be

$$\begin{array}{ccccccccc} & & \overset{\alpha_{n-1}}{\rightleftharpoons} & & \overset{\alpha_{n-2}}{\rightleftharpoons} & & \overset{\alpha_2}{\rightleftharpoons} & \overset{\alpha_1}{\rightleftharpoons} & \\ X_n & & \underset{\beta_{n-1}}{\rightleftharpoons} & X_{n-1} & \underset{\beta_{n-2}}{\rightleftharpoons} & \cdots & \underset{\beta_2}{\rightleftharpoons} & X_2 \underset{\beta_1}{\rightleftharpoons} & X_1 \\ \epsilon_n \uparrdownarrow \omega_n & & \epsilon_{n-1} \uparrdownarrow \omega_{n-1} & & & & \epsilon_2 \uparrdownarrow \omega_2 & \epsilon_1 \uparrdownarrow \omega_1 & \\ & & \overset{\alpha'_{n-1}}{\rightleftharpoons} & & \overset{\alpha'_{n-2}}{\rightleftharpoons} & & \overset{\alpha'_2}{\rightleftharpoons} & \overset{\alpha'_1}{\rightleftharpoons} & \\ X'_n & & \underset{\beta'_{n-1}}{\rightleftharpoons} & X'_{n-1} & \underset{\beta'_{n-2}}{\rightleftharpoons} & \cdots & \underset{\beta'_2}{\rightleftharpoons} & X'_2 \underset{\beta'_1}{\rightleftharpoons} & X'_1 \end{array} \qquad \text{(E)}$$

To preserve the Q vs. V relationship, $\alpha_i/\beta_i = \alpha'_i/\beta'_i$. This condition together with consideration of microscopic reversibility for each circular path requires that ϵ_i/ω_i be the same for all values of i. In the simplest case the individual rate constants ϵ_i and ω_i would each be the same for all values of i. Allowing voltage dependence of ϵ and ω, scheme E would then represent a voltage- and time-dependent transition of the overall Na channel gating mechanism between two parallel sets of states. Admitting more than one parallel set of states for a channel might decrease the number of sequential states required in each set to describe channel behavior. At present there appear to be too many free parameters to distinguish models with parallel sets of states from models having only a single but likely more complex set of sequential states.

We thank Dr. C. Bergman for stimulating discussion during the course of this work and for help in some experiments. Dr. Schneider is grateful to Dr. Bergman and Dr. P. Ascher for their hospitality during his stay at the Laboratoire de Neurobiologie, Ecole Normale Supérieure, and to Drs. C. M. Armstrong and T. Begenisich for helpful discussion of kinetic models for Na channels. We thank Drs. Armstrong and W. F. Gilly for providing the computer program for their Na channel model (1979) and Dr. W. Nonner for a preprint of his paper (1980).
MFS was supported by Research Career Development Award KO5-NS00078 from the U. S. Public Health Service.

Received for publication 5 June 1981 and in revised form 5 November 1981.

REFERENCES

ADRIAN, R. H. 1978. Charge movement in the membrane of striated muscle. *Annu. Rev. Biophys. Bioeng.* **7**:85–112.

ALMERS, W. 1978. Gating currents and charge movements in excitable membranes. *Rev. Physiol. Biochem. Pharmacol.* **82**:97–190.

ARMSTRONG, C. M. 1978. Models of gating current and sodium conductance inactivation. *In* Biophysical Aspects of Cardiac Muscle. M. Morad, editor. Academic Press, Inc., New York. 75–88.

ARMSTRONG, C. M., and F. BEZANILLA. 1973. Currents related to movement of the gating particules of the sodium channels. *Nature* (*Lond.*). **242**:459–461.

ARMSTRONG, C. M., and F. BEZANILLA. 1974. Charge movement associated with the opening and closing of the activation gates of the Na channels. *J. Gen. Physiol.* **63**:533–552.

ARMSTRONG, C. M., and F. BEZANILLA. 1977. Inactivation of the sodium channel. II. Gating current experiments. *J. Gen. Physiol.* **70**:567–590.

ARMSTRONG, C. M., and W. F. GILLY. 1979. Fast and slow steps in the activation of sodium channels. *J. Gen. Physiol.* **74**:691–711.

BAUMANN, G., and G. S. EASTON. 1981. Process characterization of a single aggregation gating site. *Biophys. J.* **33**:123*a*.

BERGMAN, C., J. M. DUBOIS, E. ROJAS, and W. RATHMAYER. 1976. Decreased rate of sodium conductance inactivation in the node of Ranvier induced by a polypeptide toxin from sea anemone. *Biochem. Biophys. Acta.* **455**:173–184.

BERNARD, P., F. COURAUD, and S. LISSITZKY. 1977. Effects of a scorpion toxin from androctonus australis venom on action potential of neuroblastoma cells in culture. *Biochem. Biophys. Res. Commun.* **77**:782–788.

BEZANILLA, F., and C. M. ARMSTRONG. 1975*a*. Kinetic properties and inactivation of the gating currents of sodium channels in squid axon. *Phil. Trans. Roy. Soc. Lond. B Biol. Sci.* **270**:449–458.

BEZANILLA, F., and C. M. ARMSTRONG. 1975*b*. Properties of the sodium channel gating current. *Cold Spring Harbor Symp. Quant. Biol.* **40**:297–304.

BULLOCK, J. O., and C. L. SCHAUF. 1978. Combined voltage-clamp and dialysis of *Myxicola* axons: behaviour of membrane asymmetry currents. *J. Physiol. (Lond.)*. **378**:309–324.

BULLOCK, J. O., and C. L. SCHAUF. 1979. Immobilization of intramembrane charge in *Myxicola* giant axons. *J. Physiol. (Lond.)*. **286**:157–171.

CAHALAN, M. D., and W. ALMERS. 1979. Interactions between quaternary lidocaine, the sodium channel gates, and tetrodotoxin. *Biophys. J.* **27**:39–56.

CHIU, S. Y. 1977. Inactivation of sodium channels: second order kinetics in myelinated nerve. *J. Physiol. (Lond.)*. **273**:573–576.

DROUIN, H., and B. NEUMCKE. 1974. Specific and unspecific charges of the sodium channels of the nerve membrane. *Pfluegers Arch. Eur. J. Physiol.* **351**:207–229.

DUBOIS, J. M., and C. BERGMAN. 1975. Cesium induced rectifications in frog myelinated fibres. *Pfluegers Arch. Eur. J. Physiol.* **355**:361–364.

DUBOIS, J. M., and C. BERGMAN. 1977*a*. The steady-state potassium conductance of the Ranvier node at various external K-concentrations. *Pfluegers Arch. Eur. J. Physiol.* **370**:185–194.

DUBOIS, J. M., and C. BERGMAN. 1977*b*. Asymmetrical currents and sodium currents in Ranvier nodes exposed to DDT. *Nature (Lond.)*. **266**:741–741.

DUBOIS, J. M., and M. F. SCHNEIDER. 1981. Block of Na current and intra-membrane charge movement in myelinated nerve fibres poisoned with a vegetable toxin. *Nature (Lond.)*. **289**:685–688.

GOLDMAN, L., and R. HANIN. 1978. Initial conditions and the kinetics of the sodium conductance in *Myxicola* giant axons. II. Relaxation experiments. *J. Gen. Physiol.* **72**:879–898.

HILLE, B. 1967. The selective inhibition of delayed potassium currents in nerve by tetraethylammonium ion. *J. Gen. Physiol.* **50**:1287–1302.

HODGKIN, A. L., and A. F. HUXLEY. 1952. A quantitative description of membrane current and its application to conduction and excitation in nerve. *J. Physiol. (Lond.)*. **117**:500–544.

HOROWICZ, P., and M. F. SCHNEIDER. 1981*a*. Membrane charge movement in contracting and non-contracting skeletal muscle fibres. *J. Physiol. (Lond.)*. **314**:565–593.

HOROWICZ, P., and M. F. SCHNEIDER. 1981*b*. Membrane charge moved at contraction thresholds in skeletal muscle fibres. *J. Physiol. (Lond.)*. **314**:595–633.

KEYNES, R. D. 1980. The asymmetry current in the squid giant axon. *Proc. Int. Union Physiol. Sci.* **14:**160.

KEYNES, R. D., and E. ROJAS. 1974. Kinetics and steady-state properties of the charged system controlling sodium conductance in the squid giant axon. *J. Physiol. (Lond.).* **239:**393–434.

KEYNES, R. D., and E. ROJAS. 1976. The temporal and steadystate relationships between activation of the sodium conductance and movement of the gating particles in the squid giant axon. *J. Physiol. (Lond.).* **255:**157–189.

KOPPENHÖFER, E. 1967. Die Wirfung von Tetraäthylammonium chloride auf die Membranströme Ranvierscher Schnürringe von *Xenopus laevis*. *Pfluegers Arch. Eur. J. Physiol.* **293:**34–55.

MEVES, M. 1974. The effect of holding potential on the asymmetry currents in squid giant axons. *J. Physiol. (Lond.).* **243:**847–867.

NEUMCKE, B., W. NONNER, and R. STÄMPFLI. 1976. Asymmetrical displacement current and its relation with the activation of sodium current in the membrane of frog myelinated nerve. *Pfluegers Arch. Eur. J. Physiol.* **363:**193–203.

NONNER, W. 1969. A new voltage clamp method for Ranvier nodes. *Pfluegers Arch. Eur. J. Physiol.* **309:**116–192.

NONNER, W. 1980. Relations between the inactivation of Na channels and the immobilization of gating charge in frog myelinated nerve. *J. Physiol. (Lond.).* **299:**573–603.

NONNER, W., E. ROJAS, and R. STÄMPFLI. 1975. Displacement currents in the node of Ranvier. *Pfluegers Arch. Eur. J. Physiol.* **354:**1–18.

NONNER, W., E. ROJAS, and R. STÄMPFLI. 1978. Asymmetrical displacement current in the membrane of frog myelinated nerve: early time course and effects of membrane potential. *Pfluegers Arch. Eur. J. Physiol.* **375:**75–85.

OXFORD, G. S. 1981. Some kinetic and steady-state properties of sodium channels after removal of inactivation. *J. Gen. Physiol.* **77:**1–22.

ROMEY, G., J. P. ABITA, H. SCHWEITZ, G. WUNDERER, and M. LAZDUNSKI. 1976. Sea anemone toxin: a tool to study molecular mechanisms of nerve conduction and excitation secretion coupling. *Proc. Natl. Acad. Sci. U. S. A.* **73:**4055–4059.

SCHAUF, C. L., J. O. BULLOCK, and T. L. PENCEK. 1977. Characteristics of sodium tail currents in *Myxicola* axons. *Biophys. J.* **19:**7–28.

SCHNEIDER, M. F., and W. K. CHANDLER. 1973. Voltage-dependent charge movement in skeletal muscle: a possible step in excitation contraction coupling. *Nature (Lond.).* **242:**244–246.

SCHNEIDER, M. F., and J. M. DUBOIS. 1981. ON and OFF kinetics of intra-membrane charge movement in node of Ranvier. Abstr. VII Internat. Biophys. Cong. 333.

STÄMPFLI, R. 1974. Intraaxonal iodate inhibits sodium inactivation. *Experimentia.* **30:**505–508.

YEH, J., and C. M. ARMSTRONG. 1978. Immobilization of gating charge by a substance that simulates inactivation. *Nature (Lond.).* **273:**387–389.